Journal of Soils and Sediments (2022) 22:272–292
https://doi.org/10.1007/s11368-021-03074-y

SOILS, SEC 5 • SOIL AND LANDSCAPE ECOLOGY • RESEARCH ARTICLE

Regional soil salinity spatiotemporal dynamics and improved temporal stability analysis in arid agricultural areas

Guanfang Sun[1] · Yan Zhu[1] · Ming Ye[2] · Yang Yang[1] · Jinzhong Yang[1] · Wei Mao[1] · Jingwei Wu[1]

Received: 13 July 2021 / Accepted: 21 September 2021 / Published online: 2 October 2021

Abstract

Purpose Monitoring and evaluating spatiotemporal dynamics of soil salinity over large areas for an extended period is important for keeping crop yield in salt-affected areas, but difficult due to its high variability. In this study, measurements of soil salinity with 68 sampling sites at different depth from top soil to 1.8 m were carried out in 2017–2018 to understand soil salinity variability and temporal stability at an agricultural area (> 80 km^2).

Methods The spatial variability and mean of soil salinity was estimated by the geostatistical analysis and temporal stability analysis, respectively. Then, improved temporal stability analysis was proposed by dividing samples into 7 groups, and mean soil salinity in each group was estimated by temporal stability analysis. Lastly, monitoring network was recommended to evaluate long-term soil salinity.

Results and discussion Strong spatial dependency of soil salinity was found with most degree of spatial dependence smaller than 25%. The temporal stability analysis was difficult to choose the representative sites due to large range of mean relative difference and standard deviation of relative difference of soil salinity. The predictions of improved temporal stability analysis were significantly improved with mean relative error of soil salinity means ranging from − 2.72 to 1.61%, and determination coefficient more than 0.90. Spatial distribution of soil salinity determined by 32 long-term soil salinity monitoring locations was consistent with that of all 68 sampling locations.

Conclusion The improved temporal stability analysis combined with geostatistical analysis can obtain spatial pattern and spatial mean of regional soil salinity, and improve monitoring efficiency greatly.

Keywords Regional soil salinity variability · Arid agricultural area · Temporal stability analysis · Geostatistical analysis · Spatial mean of soil salinity

1 Introduction

Soil salinization is a major environmental and ecological concern to sustainability of agro-ecosystems, especially in arid agricultural areas with shallow water table depth (Foley et al. 2005; Singh 2015; Sun et al. 2019; Wichelns and Oster 2006). Complicated hydrogeological conditions and anthropogenic activities (e.g., soil characteristics, crop types, and irrigation schedules) in agricultural areas increase spatiotemporal variability of soil salinity (Daliakopoulos et al. 2016; Ren et al. 2016; Sylla et al. 1995). Due to the high spatiotemporal variability, it is difficult to effectively monitor, accurately estimate, and reliably predict spatiotemporal distribution of soil salinity for agricultural management (Corwin et al. 2006; Ding and Yu 2014; Hajrasuliha et al. 1980).

There have many studies focusing on using geostatistical methods to investigating the spatial and/or temporal variability of soil salinity at the field scale (Douaik et al. 2005, 2007; Li et al. 2013; Panagopoulos et al. 2006; Scudiero et al. 2017; Sylla et al. 1995; Utset et al. 1998). Sylla et al. (1995) studied spatial variability of soil salinity and its major impact factors at three study sites with areas ranging from 4 to 14.4 ha. Panagopoulos

Responsible editor: Lu Zhang

✉ Yan Zhu
zyan0701@163.com

1 State Key Laboratory of Water Resources and Hydropower Engineering Science, Wuhan University, Wuhan 430072, Hubei, China

2 Department of Earth, Ocean, and Atmospheric Science, Florida State University, Tallahassee, FL 32306, USA

et al. (2006) analyzed spatial variation of soil salinity at an experimental block (0.22 ha) and its effects on lettuce production. Douaik et al. (2005) investigated spatiotemporal variability of soil salinity within soil depth of 0—0.4 m at a site of 25 ha in Great Hungarian Plain of Hungary. Zheng et al. (2009) assessed spatiotemporal changes of soil salinity using monitoring data in a drip-irrigated field at a 54-ha cotton field located in Xinjiang, China. Gasch et al. (2015) evaluated soil electrical conductivity spatiotemporal dynamic using data sets collected in a 37-ha farm located near Pullman, Washington, USA. These studies concern spatiotemporal variability of soil salinity at sites of small areas.

At the regional scale, attentions were paid to study not only spatiotemporal variability of soil salinity but its relation with environmental factors (Abd-Elgawad et al. 2013; Bilgili 2013; Elprince 2013; Hajrasuliha et al. 1980; Hamzehpour et al. 2013; Juan et al. 2011; Navarro-Pedreño et al. 2007; Shahabi et al. 2016; Walter et al. 2001; Wang et al. 2018; Wu et al. 2014; Zare-Mehrjardi et al. 2010; Zhou et al. 2010). Walter et al. (2001) studied the spatial pattern of salinity in top soils (0–0.2 m in depth) in an area of 38,000 ha in the Chelif Valley, Algeria. Zare-Mehrjardi et al. (2010) mapped the spatial distribution of topsoil salinity, and investigated its relations with vegetation types. Wang et al. (2018) discussed spatial distribution of salt content in the top soils and its response to land use changes in an inland river watershed of China. Due to the difficulty of intensive soil sampling at the regional scale, the abovementioned studies only used the topsoil salinity data. This however is inadequate for assessing salinity variability, since land managements and agricultural activities affect salinity of both top soils and deep soils (Akramkhanov et al. 2011). Therefore, it is necessary to investigate spatiotemporal patterns of both top and deep soils for understanding soil salinity trends at the regional scales. This is one of the motivations of this study.

The soil salinity spatial pattern and mean is the major information reflecting the degree of soil salinization (Florinsky et al. 2002; Wang et al. 2017), which requires a large number of soil samples of different sites and times due to its highly spatial and temporal variability (Hajrasuliha et al. 1980). Then, sampling schemes which can reduce the sample number to represent different soil salinity levels over space are necessary. Temporal stability analysis is an effective method to characterize time-invariant associations between spatial locations and classical statistical parametric values. It can be used to identify the sampling locations to represent the spatial mean of the study area (Brocca et al. 2009; Douaik et al. 2006; Gao et al. 2013a; Hu et al. 2011; Jacobs et al. 2010; Penna et al. 2013; Vachaud et al. 1985; Vanderlinden et al. 2012). Scientific literatures showed that the concept of temporal stability analysis has been widely used to characterize the temporal stability of spatial patterns of soil moisture in different land usage types (grassland, farmlands, forest lands and agro-forest ecosystems) from field to watershed scales (Gao et al. 2013a; Guber et al. 2008; Hu et al. 2011, 2010; Lin 2006; Vachaud et al. 1985). The mean relative difference (MRD) method is one of most popular methods used for temporal stability analysis, in which the location with *MRD* closed to zero or with minimum standard deviation of relative difference (*SDRD*) is taken as representative location. The characteristics of *MRD* and *SDRD* may the key factors to impact the effectiveness of the method to find the representative locations. It was found that some locations can represent the mean water content at any time with *MRD* ranging from − 0.07 to 0.07 in an agricultural land of Sevilla in Spain (Vachaud et al. 1985). The method was successfully used to find the representative locations in four catchments with the *MRD* range from − 0.41 to 0.54 and with the largest *SDRD* of 0.30 (Grayson and Western 1998). Liu and Shao (2014) reported that the method can estimate the soil water storage well with representative locations when the maximum *SDRD* less than 0.12. Mohanty and Skaggs (2001) found that *MRD* of soil moisture can range from − 0.70 to 1.40, and *SDRD* from 0.12 to 1.00, while cautions should be paid in some areas with large range of *MRD* and *SDRD* values.

Comparing to the abundant study of temporal stability of soil moisture, knowledge on temporal stability of soil salt was limited to field scales with fewer studies reported. Castrignanò et al. (1994) evaluated the variability and temporal stability of soil salinity in a field with 2.8 ha within the depth of 0.6 m and found that the spatial mean of soil salinity can be represented by limited locations. Douaik et al. (2006) reported that a reliable average soil salinity can be obtained by observing the soil salinity of two locations in a 25-ha field within the depth of 0.4 m. Xing et al. (2015) studied the temporal stability of root zone soil salinity in an experiment plot with 12.5 m × 10 m and confirmed that temporal stability representative locations can be selected as long-term soil salt monitoring points in this field. Current studies on temporal stability of soil salinity focused on field scale, where relative smaller variations of soil salinity level were found with *MRD* values ranging from − 0.75 to 1.11 (Douaik et al. 2006; Xing et al. 2015), which help to obtain acceptable spatial mean of soil salinity by representative locations (Xing et al. 2015). However, the temporal stability analysis would be challenged in a larger scale, where owns much larger *MRD* and *SDRD* of soil salinity.

In this study, a 2-year field experiment was carried out to characterize the temporal and spatial variability of soil salinity in a relatively large irrigation area (> 80 km^2). Soil samples were collected 4 times before and after the crop growing season of 2017–2018, and there were 68 sampling sites for each time. Soil samples were collected from the top soil to the depth of 1.8 m or until the water table depth if it was shallower than 1.8 m with the interval of 0.2 m. The spatial variability of soil salinity at different depth from the top soil to 1.8 m were estimated by the geostatistical analysis. The temporal stability analysis was used to estimate and to predict the spatial mean of soil salt in the entire area, while it was found being difficult to select reasonable representative locations due to the large range of *MRD* and *SDRD*. Then, the improved temporal stability analysis was proposed to overcome shortcomings of temporal stability analysis on soil salinity, in which the soil samples were divided into several groups and the mean soil salinity of each group was estimated with representative locations by using temporal stability analysis. A monitoring network for this area was then recommended to evaluate the long-term evolution characteristics of soil salinity by comprehensively considering the results of spatiotemporal variability and the improved temporal stability analysis.

2 Material and methods

2.1 Study area and field measurements

The study area, the Longsheng irrigation district, is located in the central region of the Hetao Irrigation District in the west of Inner Mongolia Autonomous Region, China (Fig. 1). Its area is 82 km^2, 15.5 km long measured in the southwest-northeast direction and 8.0 km wide in northwest-southeast direction. Based on the weather data obtained from the Linhe Weather Station adjacent to the study area, the cumulative precipitation was 100.5 mm in 2017 and 176.2 mm in 2018. These two years were selected to represent the dry and wet years, respectively, according to a hydrological frequency analysis using precipitation data from 1981 to 2018. During the crop growing season from May to September, the cumulative precipitation was 53.1 mm in 2017 and 156.6 mm in 2018. Measurements of soil salinity were carried out 4 times during early May and late September of 2017 and 2018, and these measurement times were denoted as Y1705, Y1709, Y1805, and Y1809.

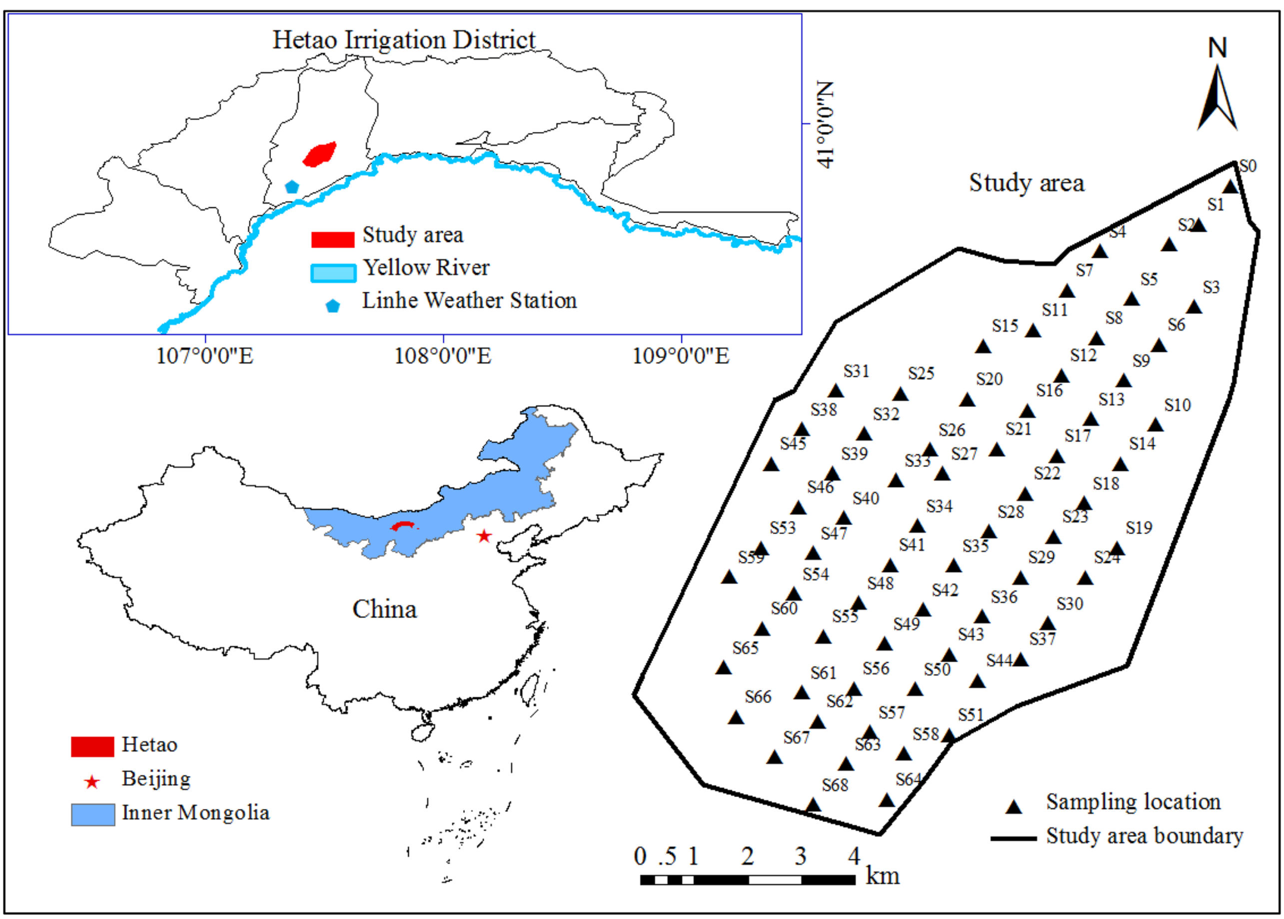

Fig. 1 Locations of the Longsheng irrigation district, and soil salinity samples in the study area

For each measurement time, 68 sampling locations were designed as shown in Fig. 1, and observations were replicated two times at each sampling location. Soil samples were collected from the top soil to the depth of 1.8 m or until the water table depth if it was shallower than 1.8 m with the interval of 0.2 m. There were a total of 4582 soil samples collected during the experiment for measuring the soil salinity. Soil salinity was determined from measurements of electrical conductivity (EC) of leaching liquid mixed with 1 (soil sample):5 (water) ratio with electrical conductivity meter (DDSJ-308F, China) (Ding and Yu 2014; Visconti et al. 2010).

2.2 Geostatistical analysis

The spatial variability and correlations of soil salinity are quantified by using the empirical semivariogram defined as (Webster and Oliver 2007; Hu et al. 2010)

$$\gamma(h) = \frac{1}{2N(h)} \sum_{i=1}^{N(h)} [Z(x_i + h) - Z(x_i)]^2, \quad (1)$$

where $\gamma(h)$ is the semivariogram; h is the lag distance; $N(h)$ is the number of pairs (x_i, $x_i + h$); $Z(x_i)$ and $Z(x_i + h)$ are values of soil salinity at positions x_i and $x_i + h$.

Three semivariogram models (i.e., spherical, exponential, and Gaussian models) have been employed to fit the empirical semivariograms, and the models are defined as follows (Zhang 2005):

$$\gamma(h) = \begin{cases} 0 & h = 0 \\ C_0 + C_1\left(\frac{3h}{2a} - \frac{h^3}{2a^3}\right) & 0 < h \le a \\ C_0 + C_1 & h > a \end{cases}, \quad (2)$$

$$\gamma(h) = \begin{cases} 0 & h = 0 \\ C_0 + C_1\left(1 - e^{-\frac{h}{a}}\right) & h > 0 \end{cases}, \quad (3)$$

$$\gamma(h) = \begin{cases} 0 & h = 0 \\ C_0 + C_1\left(1 - e^{-\frac{h^2}{a^2}}\right) & h > 0 \end{cases}, \quad (4)$$

where C_0 is the nugget variance, C_1 is the structured variance, and a is the correlation length. The correlation length is related to range R, which is a, $3a$, and $1.732a$ for the spherical, exponential, and Gaussian models, respectively. The coefficient of determination (R^2) and residual sums of squares (*RSS*) were used to assess the fitness of different semivariogram models. Models with the highest R^2 and lowest *RSS* were taken as the fitted semivariogram models (Li et al. 2020).

The nugget variance (C_0), sill variance ($C_0 + C_1$), and range R are the three geostatistical parameters in theoretical semivariogram models. The degree of spatial dependence (*GD*), which is the ratio between the nugget variance and the sill variance, was used to characterize the spatial dependency of soil salinity. $GD < 0.25$ indicates a strong spatial dependency, while $GD > 0.75$ a weak spatial dependency, otherwise a moderate spatial dependency (Li

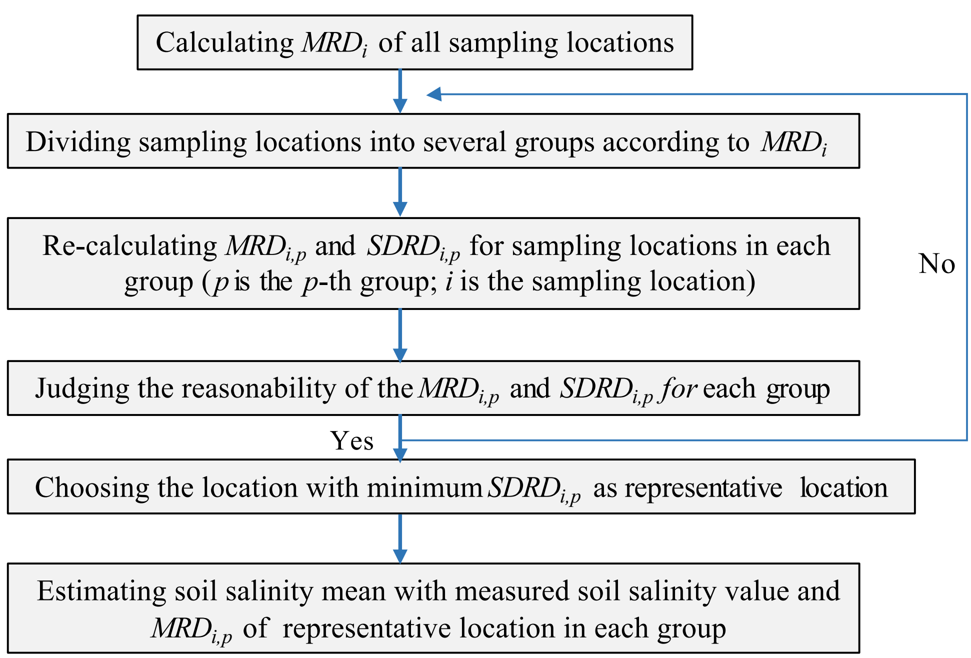

Fig. 2 Flowchart of the improved temporal stability analysis. MRD_i is the temporal mean relative difference at the sampling location i; $MRD_{i,p}$ is the *MRD* at the sampling location i in the p-th group; and $SDRD_{i,p}$ is the standard deviation of relative difference (*RD*) at the sampling location i in the p-th group

et al. 2020). The range R was used to judge the spatial autocorrelation scale of random variables.

Ordinary kriging was used to estimate the values at unsampled locations, and "leave-one-out" cross-validation was conducted on the kriging analysis (Ruybal et al. 2019). The measured and predicted soil salinity were compared for goodness of fit to assess the kriging model.

2.3 Temporal stability analysis

The MRD method was employed to study the temporal stability of soil salinity. The relative difference ($RD_{i,j}$) of the sampling time j at the sampling location i for a given depth with respect to the spatial mean soil salinity (S_j) is defined as (Vachaud et al. 1985),

Table 1 Summary statistics of soil salinity at the 4 sampling times

Sampling time	Soil layer (m)	Number	Mean (dS/m)	Median (dS/m)	*SD* (dS/m)	*CV*	Minimum (dS/m)	Maximum (dS/m)
Y1705	0–0.2	65	0.34	0.23	0.39	1.14	0.13	2.34
	0.2–0.4	65	0.30	0.25	0.18	0.60	0.12	0.99
	0.4–0.6	65	0.31	0.27	0.21	0.66	0.11	1.35
	0.6–0.8	65	0.33	0.26	0.20	0.60	0.10	1.18
	0.8–1.0	65	0.33	0.27	0.19	0.57	0.10	1.18
	1.0–1.2	64	0.31	0.26	0.16	0.52	0.06	0.90
	1.2–1.4	51	0.29	0.24	0.15	0.51	0.12	0.92
	1.4–1.6	45	0.28	0.23	0.15	0.54	0.12	0.88
	1.6–1.8	29	0.32	0.27	0.19	0.61	0.12	1.01
Y1709	0–0.2	66	0.35	0.23	0.28	0.78	0.10	1.55
	0.2–0.4	66	0.33	0.24	0.24	0.74	0.12	1.19
	0.4–0.6	66	0.32	0.26	0.20	0.63	0.07	0.96
	0.6–0.8	66	0.29	0.26	0.15	0.53	0.07	0.74
	0.8–1.0	66	0.28	0.27	0.13	0.47	0.07	0.73
	1.0–1.2	66	0.28	0.25	0.13	0.46	0.09	0.63
	1.2–1.4	66	0.26	0.24	0.12	0.44	0.09	0.68
	1.4–1.6	66	0.25	0.24	0.11	0.43	0.10	0.55
	1.6–1.8	66	0.26	0.24	0.12	0.48	0.07	0.81
Y1805	0–0.2	67	0.28	0.23	0.13	0.45	0.14	0.77
	0.2–0.4	67	0.29	0.23	0.15	0.52	0.13	0.76
	0.4–0.6	67	0.32	0.24	0.20	0.63	0.12	1.02
	0.6–0.8	67	0.33	0.26	0.20	0.61	0.12	1.03
	0.8–1.0	67	0.33	0.27	0.18	0.54	0.12	0.92
	1.0–1.2	67	0.33	0.27	0.17	0.53	0.11	0.90
	1.2–1.4	65	0.31	0.25	0.15	0.48	0.11	0.72
	1.4–1.6	64	0.29	0.24	0.13	0.46	0.14	0.78
	1.6–1.8	58	0.27	0.22	0.12	0.45	0.11	0.77
Y1809	0–0.2	66	0.28	0.20	0.21	0.77	0.08	1.29
	0.2–0.4	66	0.30	0.23	0.21	0.71	0.08	1.23
	0.4–0.6	66	0.32	0.26	0.20	0.63	0.10	1.03
	0.6–0.8	66	0.31	0.24	0.20	0.64	0.09	1.06
	0.8–1.0	66	0.29	0.22	0.17	0.61	0.09	0.89
	1.0–1.2	66	0.28	0.23	0.18	0.62	0.09	1.13
	1.2–1.4	66	0.27	0.23	0.15	0.56	0.10	0.91
	1.4–1.6	66	0.26	0.22	0.13	0.51	0.08	0.86
	1.6–1.8	66	0.25	0.23	0.12	0.47	0.08	0.65

SD standard deviation, *CV* coefficient of variation

$$RD_{i,j} = \frac{S_{i,j} - \overline{S_j}}{\overline{S_j}}, \quad (5)$$

$$\overline{S_j} = \frac{1}{n}\sum_{i=1}^{n} S_{i,j}, \quad (6)$$

where $S_{i,j}$ is the soil salinity at the location i of the sampling time j, and n is the number of sampling locations. The temporal mean relative difference MRD_i and the standard deviation of $RD_{i,j}$ at the location i ($SDRD_i$) over time are calculated as (Penna et al. 2013),

$$MRD_i = \frac{1}{m}\sum_{j=1}^{m} RD_{i,j}, \quad (7)$$

$$SDRD_i = \sqrt{\sum_{j=1}^{m} \frac{(RD_{i,j} - MRD_i)^2}{m-1}}, \quad (8)$$

where m is the total number of sampling times. MRD_i measures the bias between the observation values at the sampling location i and the spatial mean observation value over a certain period, and $SDRD_i$ quantifies accuracy of the bias measurement (Gao et al. 2013b). In our study, the sampling location with the minimum $SDRD_i$ was selected as the representative location (Brocca et al. 2009).

Rearranging Eq. (5), the spatial mean soil salinity can be expressed as

$$\overline{S_j} = \frac{S_{i,j}}{1 + RD_{i,j}}, \quad (9)$$

The offset ($RD_{i,j}$) between the representative location and the mean value can be equal to MRD_i, and the spatial mean can be estimated as (Grayson and Western 1998; Hu et al. 2010; Heathman et al. 2012; Gao et al. 2013a),

$$S_{mean,j} = \frac{S_{RL,j}}{1 + MRD_{RL}}, \quad (10)$$

where $S_{mean,j}$ is the spatial mean of soil salinity of the sampling time j, $S_{RL,j}$ is the soil salinity of representative locations, and MRD_{RL} is the temporal MRD of representative locations with the smallest $SDRD$.

2.4 Improved temporal stability analysis of soil salinity

Temporal stability analysis can provide accurate results with relatively smaller MRD ranging from −0.50 to 0.60 and most maximum $SDRD$ value being smaller than 0.50 (Brocca et al. 2009; Vanderlinden et al. 2012). Since MRD and $SDRD$ of soil salinity are much larger at this study area (shown in Sect. 3.3), the improved temporal stability analysis of soil salinity was developed to reduce MRD and $SDRD$, the procedures of which are shown in Fig. 2. The MRD method is first used to calculate MRD_i of each sampling location. Then, all sampling locations are divided into several groups according to the ranked MRD_i. The MRD method is used to calculate the $MRD_{i,p}$ and $SDRD_{i,p}$ (where p means the p-th group and i is the sampling location) of the sampling locations in each group. The reasonability of $MRD_{i,p}$ and $SDRD_{i,p}$ in each dividing group is then evaluated, and the evaluation criteria are discussed in Sect. 3.5. The sampling location with the minimum $SDRD_{i,p}$ in p-th group is selected as the representative location, and then the spatial mean soil salinity of each group is calculated by using Eq. (10).

2.5 Accuracy indictors

The mean relative error (MRE), the root mean square error ($RMSE$), and the determination coefficient (R^2) were used to evaluate the misfit between the observed and predicted soil salinity, which are defined as follows (Ren et al. 2016):

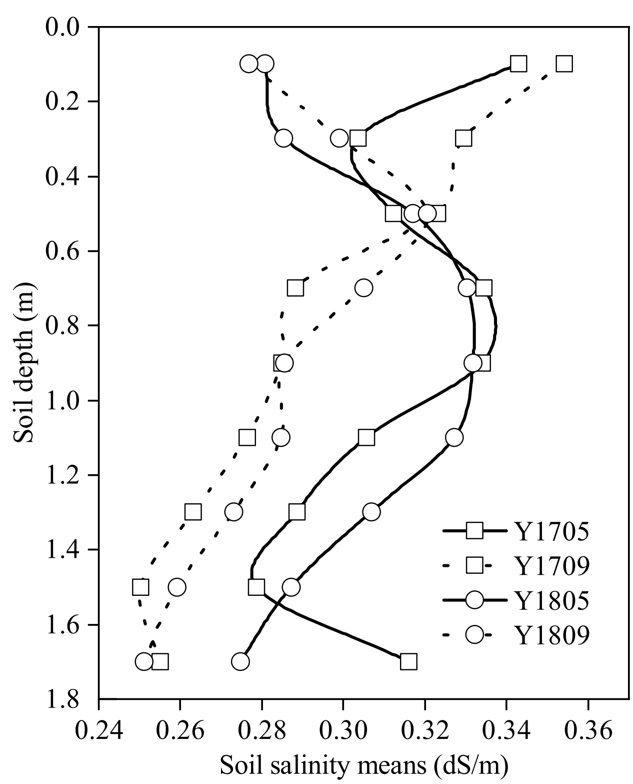

Fig. 3 The soil salinity means of different soil layers at 4 sampling times

Table 2 The semivariogram models and prediction accuracy of soil salinity at the 4 sampling times

Time	Soil layer (m)	Model	C_0	C_0+C_1	$C_0/(C_0+C_1)$	R (m)	*MRE* (%)	*RMSE* (dS/m)
Y1705	0–0.2	Spherical	0.0160	0.3480	4.60	1440	6.96	0.41
	0.2–0.4	Gaussian	0.0422	0.2604	16.21	1542	1.88	0.18
	0.4–0.6	Spherical	0.0020	0.2762	0.72	1610	1.66	0.21
	0.6–0.8	Exponential	0.0844	0.3078	27.42	6150	1.89	0.19
	0.8–1.0	Exponential	0.0527	0.2654	19.86	3990	1.20	0.18
	1.0–1.2	Spherical	0.0080	0.2280	3.51	1600	1.75	0.16
	1.2–1.4	Spherical	0.0083	0.1916	4.33	1440	3.57	0.16
	1.4–1.6	Spherical	0.0091	0.2232	4.08	1400	3.94	0.16
	1.6–1.8	Spherical	0.0182	0.2574	7.07	1200	4.90	0.21
Y1709	0–0.2	Exponential	0.0450	0.3770	11.94	1500	4.25	0.28
	0.2–0.4	Exponential	0.0389	0.3328	11.69	1680	4.05	0.25
	0.4–0.6	Gaussian	0.0407	0.3294	12.36	1697	-0.23	0.21
	0.6–0.8	Exponential	0.0404	0.2928	13.80	2790	-0.08	0.15
	0.8–1.0	Spherical	0.1301	0.4102	31.72	19,020	0.16	0.12
	1.0–1.2	Gaussian	0.1456	0.2922	49.83	12,679	0.38	0.12
	1.2–1.4	Exponential	0.1176	0.3752	31.34	47,280	0.55	0.11
	1.4–1.6	Exponential	0.1335	0.2680	49.81	32,220	0.28	0.11
	1.6–1.8	Spherical	0.1644	0.3298	49.85	20,340	0.10	0.12
Y1805	0–0.2	Gaussian	0.0001	0.1532	0.07	1403	1.32	0.14
	0.2–0.4	Gaussian	0.0011	0.1972	0.56	1472	2.22	0.15
	0.4–0.6	Gaussian	0.0010	0.2902	0.34	1801	0.23	0.20
	0.6–0.8	Exponential	0.0111	0.2942	3.77	3780	0.19	0.19
	0.8–1.0	Spherical	0.1046	0.2692	38.86	7220	1.77	0.15
	1.0–1.2	Exponential	0.0506	0.2612	19.37	5250	1.66	0.15
	1.2–1.4	Exponential	0.0375	0.1990	18.84	3480	0.72	0.12
	1.4–1.6	Exponential	0.0285	0.1740	16.38	3630	1.18	0.11
	1.6–1.8	Spherical	0.0580	0.1710	33.92	2470	0.98	0.11
Y1809	0–0.2	Exponential	0.1390	0.8050	17.27	63,300	4.73	0.21
	0.2–0.4	Exponential	0.1280	0.5510	23.23	36,600	3.90	0.20
	0.4–0.6	Exponential	0.0478	0.3466	13.79	6810	2.75	0.17
	0.6–0.8	Spherical	0.1350	0.4580	29.48	12,090	1.27	0.17
	0.8–1.0	Spherical	0.1301	0.3602	36.12	9950	1.54	0.14
	1.0–1.2	Exponential	0.0799	0.2918	27.38	8580	1.65	0.14
	1.2–1.4	Spherical	0.1225	0.2550	48.04	5570	1.62	0.13
	1.4–1.6	Spherical	0.1063	0.2136	49.77	6210	1.32	0.11
	1.6–1.8	Exponential	0.0366	0.1962	18.65	3930	1.26	0.10

The mean relative error (*MRE*) and root mean square error (*RMSE*) indicate accuracy of kriging interpolation

C_0 nugget variance, C_0+C_1 sill variance, $C_0/(C_0+C_1)$ degree of spatial dependence (%), R range

$$MRE = \frac{1}{k}\sum_{i=1}^{k}\frac{P_i - O_i}{O_i} \times 100\%, \tag{11}$$

$$RMSE = \sqrt{\frac{1}{k}\sum_{i=1}^{k}(P_i - O_i)^2}, \tag{12}$$

$$R^2 = \left[\frac{\sum_{i=1}^{k}(O_i - \overline{O})(P_i - \overline{P})}{\left[\sum_{i=1}^{k}(O_i - \overline{O})^2\right]^{0.5}\left[\sum_{i=1}^{k}(P_i - \overline{P})^2\right]^{0.5}}\right]^2, \tag{13}$$

where k is the total number of observations; P_i and O_i are the predicted and observed values ($i = 1, 2, \ldots, n$); $\overline{O}$ and $\overline{P}$ are the mean observations and predictions.

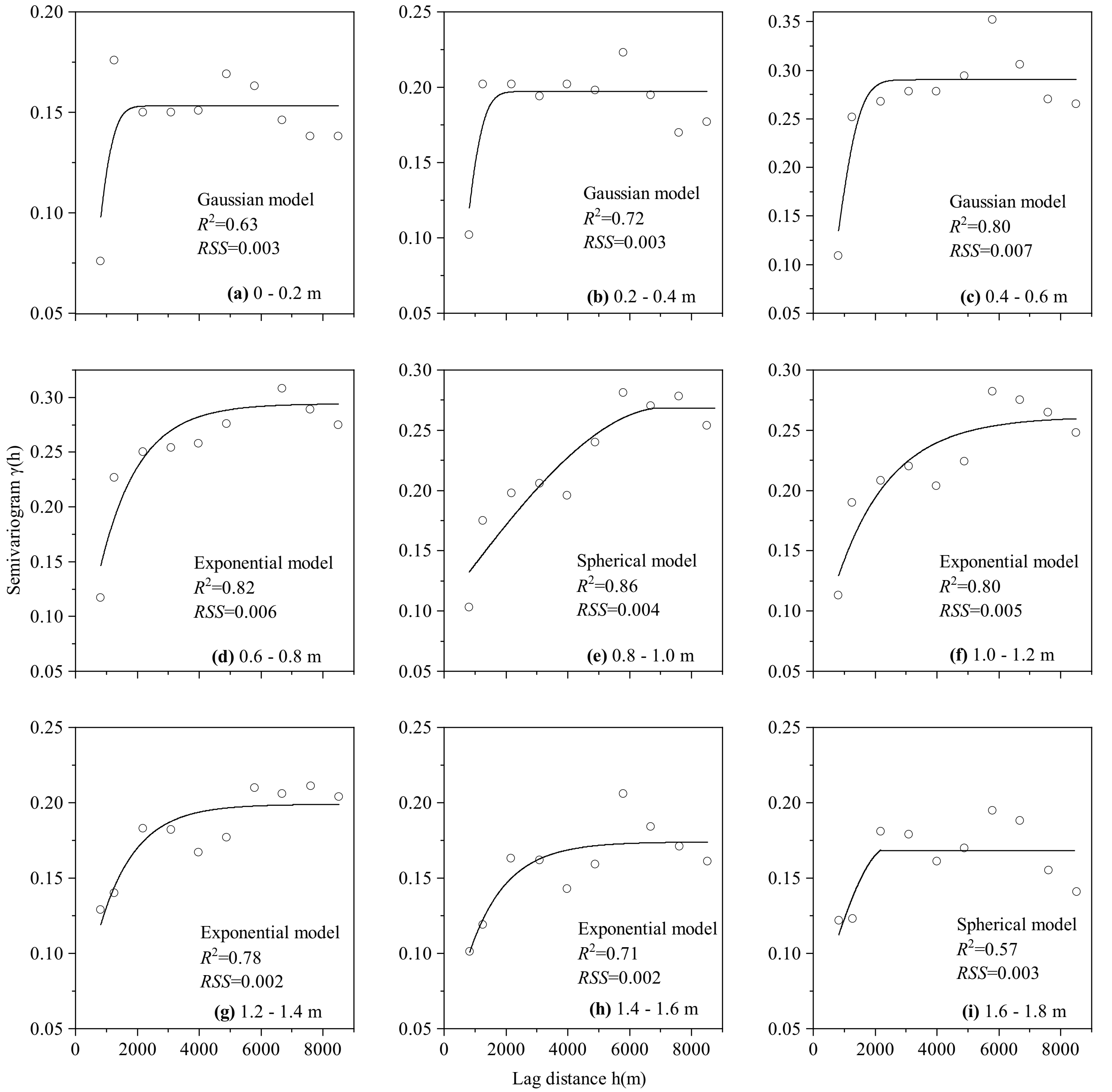

Fig.4 Experimental (circles) and theoretical (lines) semivariogram of soil salinity for various soil depths in Y1805

3 Results and discussion

3.1 Summary statistics of soil salinity

Summary statistics of soil salinity at various soil layers at the 4 sampling times are listed in Table 1. Generally speaking, the maximum values are about one order of magnitude larger than the minimum values, and the spatial variability of soil salinity is high with the coefficients of variation (CV) ranging from 0.43 to1.14. According to Warrick and Nielsen (1980), $0.1 \leq CV \leq 1.0$ indicates moderate variability, and $CV > 1.0$ strong variability.

The spatial mean of soil salinity of the 4 sampling times at various depths is presented in Fig. 3. Although the soil salinity within the topsoil was distinctly impacted by upper boundary conditions (e.g., irrigation, precipitation), the soil salinity within the depth of 0–0.6 m (the root zone) in September was larger than that in May, the

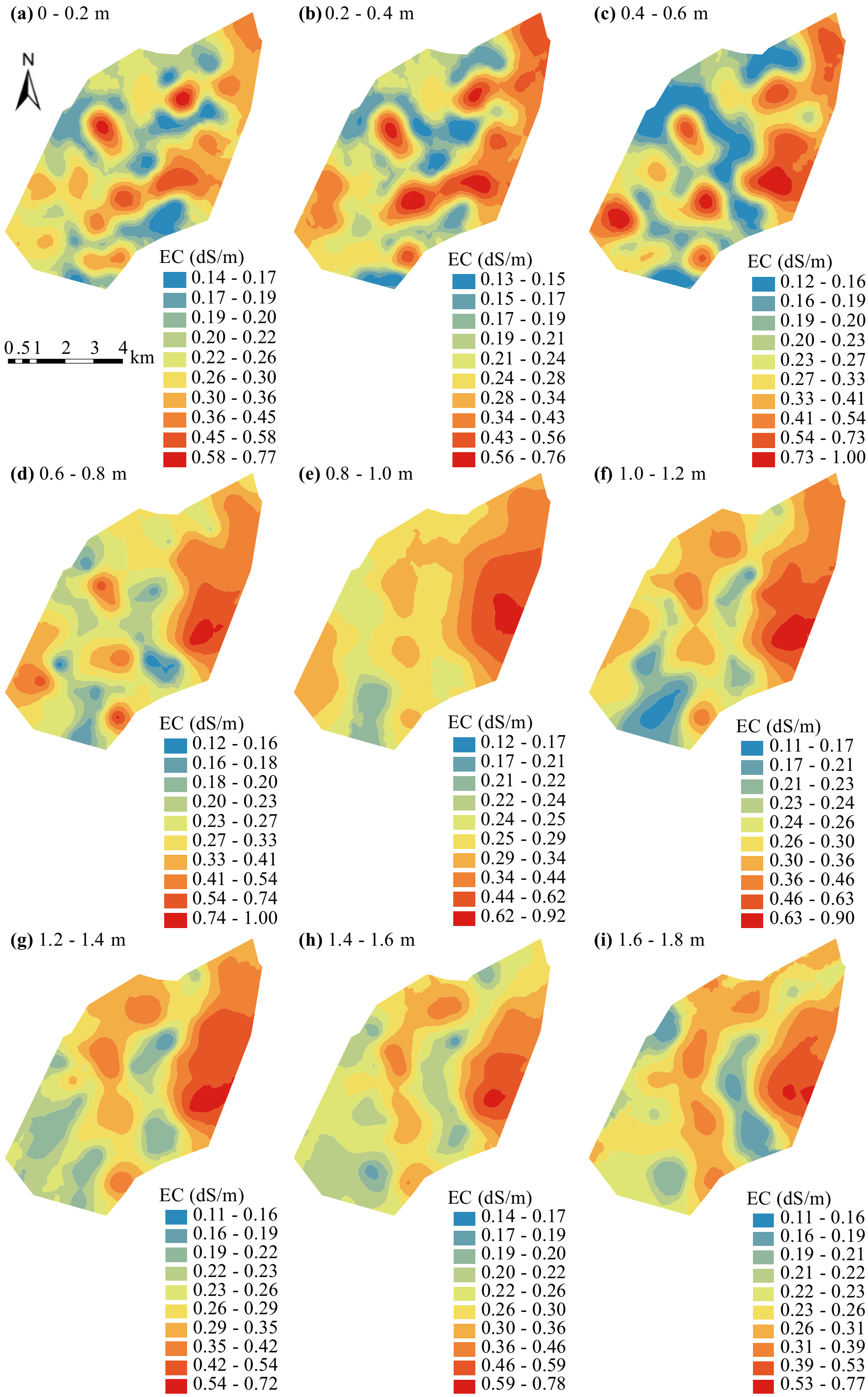

Fig. 5 The spatial distribution of soil salinity of different soil layers in Y1805

values of which were 0.32 dS/m, 0.34 dS/m, 0.29 dS/m, and 0.30 dS/m in Y1705, Y1709, Y1805, and Y1809. Heavy precipitation can help to leach soil salt out effectively, which can be found in Fig. 3 that the soil salinity within the depth of 0–0.6 m in Y1709 was larger than that in Y1809. And the soil salinity within the depth of 0.6–1.8 m was smaller in September than in May, the values of which were 0.30 dS/m, 0.27 dS/m, 0.31 dS/m, and 0.28 dS/m in Y1705, Y1709, Y1805, and Y1809. During the crop growing season from May to September, soil salts mainly move upwards from the deep soil layer (within the depth of 0.6–1.8 m) to the root zone caused by the shallow groundwater table depth and strong evapotranspiration. This is the major reason to result in the smaller soil salinity in the deep soil layer in September than that in May. All these demonstrate that the soil salinity has obvious seasonal variation characteristics although the upper boundary conditions are inconsistent in 2017 and 2018.

Fig. 7 The mean relative difference (*MRD*) and standard deviation of relative difference (*SDRD*) of soil salinity, and the S38, S45, S5, S64, S39, and S44 are representative locations with the minimum *SDRD* ▸

3.2 Spatiotemporal pattern of soil salinity

The spatial pattern of soil salinity at different soil layers was analyzed by the semivariogram models, which are listed in Table 2. And experimental and theoretical semivariogram of soil salinity for various soil depths in Y1805 are plotted in Fig. 4. It can be found that the spherical,

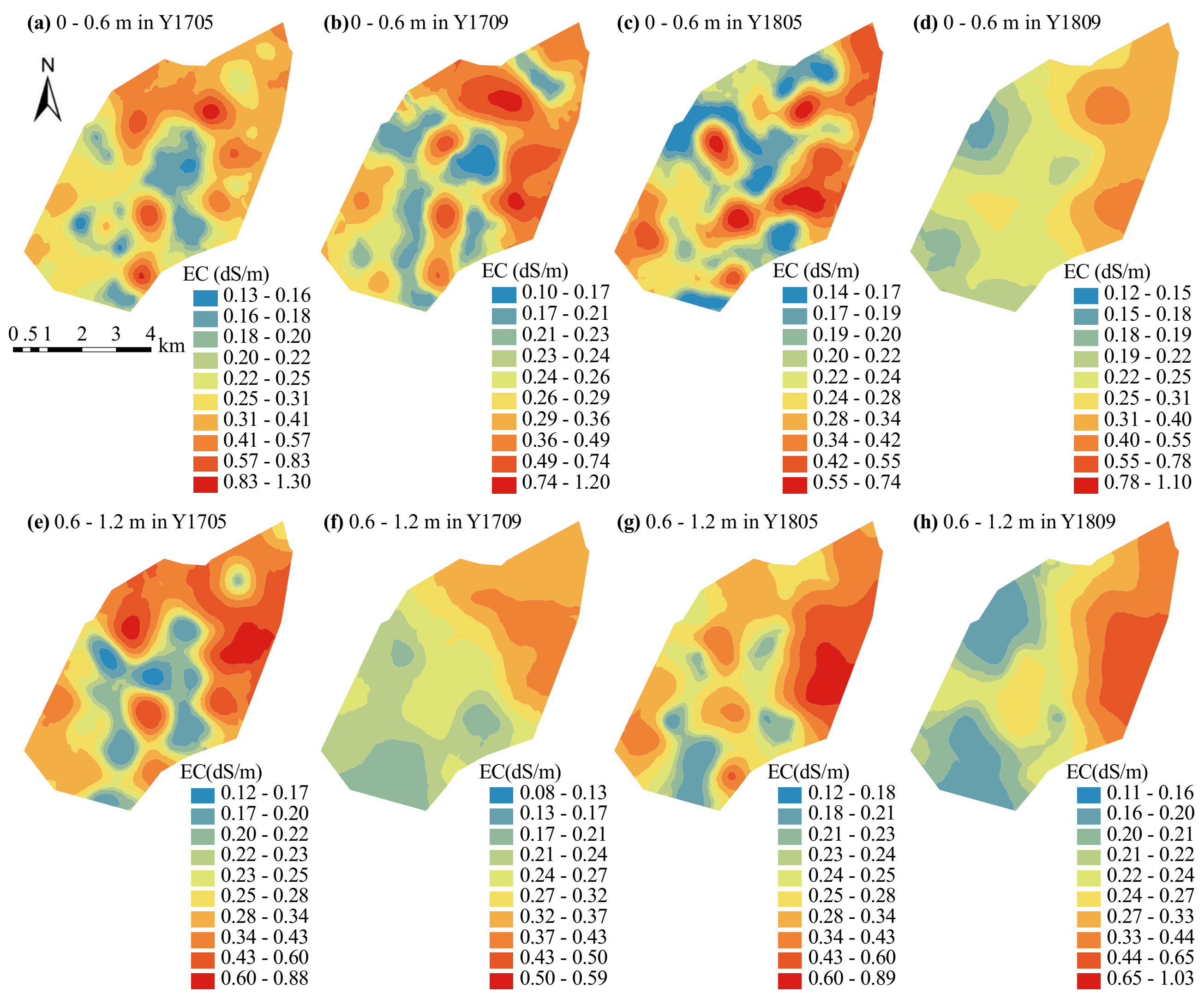

Fig. 6 The soil salinity spatial distribution of root zone (within the depth of 0–0.6 m) and 0.6–1.2 m layer at the 4 sampling times

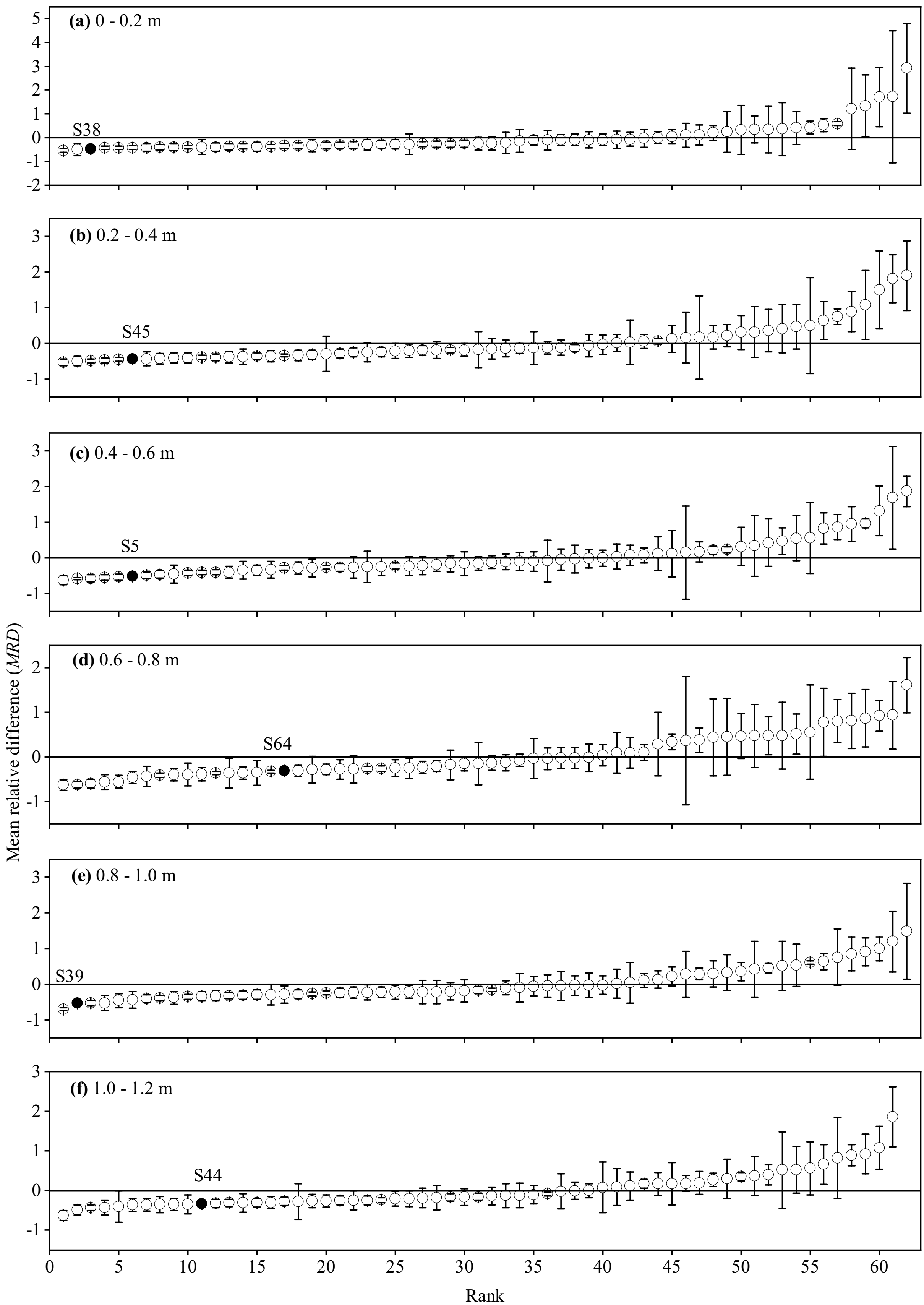

(a) 0 - 0.2 m
S38
(b) 0.2 - 0.4 m
S45
(c) 0.4 - 0.6 m
S5
(d) 0.6 - 0.8 m
S64
(e) 0.8 - 1.0 m
S39
(f) 1.0 - 1.2 m
S44
Mean relative difference (MRD)
Rank

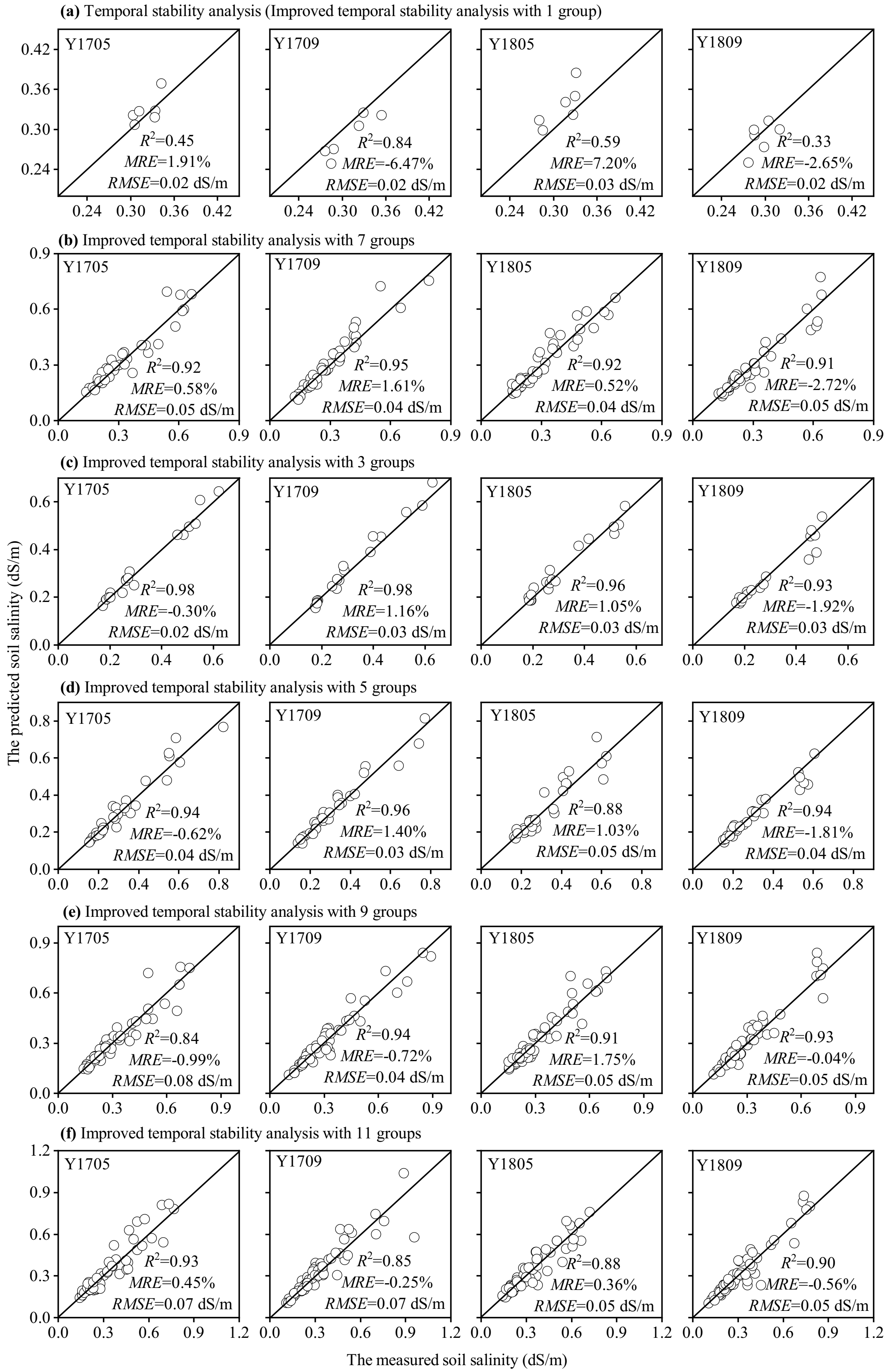
(a) Temporal stability analysis (Improved temporal stability analysis with 1 group)
Y1705
R2=0.45
MRE=1.91%
RMSE=0.02 dS/m
Y1709
R2=0.84
MRE=-6.47%
RMSE=0.02 dS/m
Y1805
R2=0.59
MRE=7.20%
RMSE=0.03 dS/m
Y1809
R2=0.33
MRE=-2.65%
RMSE=0.02 dS/m
(b) Improved temporal stability analysis with 7 groups
Y1705
R2=0.92
MRE=0.58%
RMSE=0.05 dS/m
Y1709
R2=0.95
MRE=1.61%
RMSE=0.04 dS/m
Y1805
R2=0.92
MRE=0.52%
RMSE=0.04 dS/m
Y1809
R2=0.91
MRE=-2.72%
RMSE=0.05 dS/m
(c) Improved temporal stability analysis with 3 groups
Y1705
R2=0.98
MRE=-0.30%
RMSE=0.02 dS/m
Y1709
R2=0.98
MRE=1.16%
RMSE=0.03 dS/m
Y1805
R2=0.96
MRE=1.05%
RMSE=0.03 dS/m
Y1809
R2=0.93
MRE=-1.92%
RMSE=0.03 dS/m
(d) Improved temporal stability analysis with 5 groups
Y1705
R2=0.94
MRE=-0.62%
RMSE=0.04 dS/m
Y1709
R2=0.96
MRE=1.40%
RMSE=0.03 dS/m
Y1805
R2=0.88
MRE=1.03%
RMSE=0.05 dS/m
Y1809
R2=0.94
MRE=-1.81%
RMSE=0.04 dS/m
(e) Improved temporal stability analysis with 9 groups
Y1705
R2=0.84
MRE=-0.99%
RMSE=0.08 dS/m
Y1709
R2=0.94
MRE=-0.72%
RMSE=0.04 dS/m
Y1805
R2=0.91
MRE=1.75%
RMSE=0.05 dS/m
Y1809
R2=0.93
MRE=-0.04%
RMSE=0.05 dS/m
(f) Improved temporal stability analysis with 11 groups
Y1705
R2=0.93
MRE=0.45%
RMSE=0.07 dS/m
Y1709
R2=0.85
MRE=-0.25%
RMSE=0.07 dS/m
Y1805
R2=0.88
MRE=0.36%
RMSE=0.05 dS/m
Y1809
R2=0.90
MRE=-0.56%
RMSE=0.05 dS/m
The predicted soil salinity (dS/m)
The measured soil salinity (dS/m)

◂**Fig. 8** The measured and predicted mean soil salinity of each soil layer within the depth of 0–1.2 m by the temporal stability analysis and improved temporal stability analysis, and the line is 1:1

exponential, and Gaussian models can fit the empirical semivariograms well, with most values of R^2 greater than 0.70 and most *RSS* smaller than 0.003. The degree of spatial dependence of soil salinity ranged from 0.07% to 49.85% with most smaller than 25%, which shows strong spatial dependency in the study area. The degree of spatial dependence at the end of the crop growing season (Y1709 and Y1809) were obviously greater than that at the beginning of growing season (Y1705 and Y1805). The average *R* values within the depth of 0–0.6 m were 1448 m, 1535 m, and 1703 m in Y1705, Y1709, and Y1805. The *R* value of soil salinity within the depth of 0–0.6 m was more than 6180 m in Y1809, which was evidently larger than those in other sampling times. It may be caused by the precipitation event happening before the sampling time that increases the spatial homogeneity of root zone soil salt. The range *R* values in 0.6–1.8 m were greater at the end of crop growing season (Y1709 and Y1809) than that at the beginning of crop growing season (Y1705 and Y1805). It is consistent with the law that the soil salinity with larger spatial mean own stronger variability (Table 1). Regardless of the maximum and minimum values, the average *R* values of 0.6–0.8 m, 0.8–1.0 m, 1.0–1.2 m, 1.2 m–1.4 m, 1.4–1.6 m, and 1.6–1.8 m were 4965 m, 8585 m, 6915 m, 4525 m, 4920 m, and 3200 m. It means that the sampling interval of soil salinity of 0–0.6 m should be smaller than 1448 m, and 0.6–1.8 m can be 3200 m when using *R* as a reference for determining sampling locations.

As shown in Table 2, the spatial structure characteristics of soil salinity were different at the 4 sampling times, which are highly influenced by natural and human factors. It also implies that it is not reliable to obtain the spatial structure characteristics of soil salinity by results of single sampling time, while results of multi sampling times are needed to figure out the spatial structure characteristics of soil salinity for determining the appropriate sampling locations.

Based on the semivariograms analysis, the spatial distribution of soil salinity at different soil layers at the 4 sampling times was estimated using the ordinary kriging method (Zhang 2005), and results of "leave-one-out" cross-validation are listed in Table 2. Figure 5 shows the spatial distribution of soil salinity of different soil layers in Y1805. The distribution of high and low values of soil salinity in different soil layers are highly related. The location and size of patches with same color of each layer within the depth of 0–0.6 m were almost identical, and very similar distribution patterns were found in each layer within the depth of 0.6–1.8 m, which indicate that the soil salinity is closely related to each other in different depths. The soil salinity spatial distributions within the depths of 0–0.6 m (the root zone) and 0.6–1.2 m at the 4 sampling times are shown in Fig. 6. The soil salinity in the eastern and northeast part of the study area was always higher than that in the north and south parts. Very small changes of spatial distribution pattern were found with time. These show that the spatial patterns of soil salinity are relatively stable in time. The spatiotemporal pattern of soil salinity in this study area demonstrates that it is not necessary to monitor soil salinity of deep layer due to similar spatial pattern of different soil layers being found, and monitoring frequency can also be decreased due to its temporal stability.

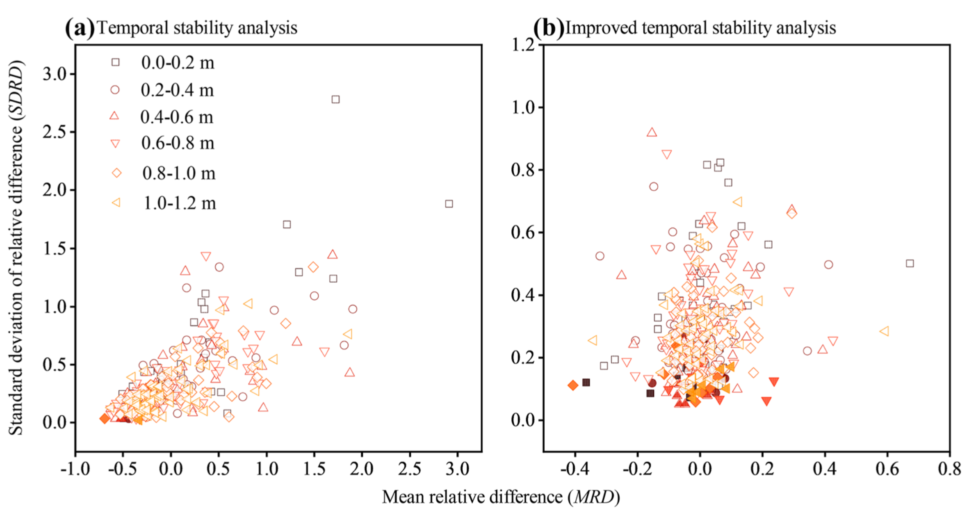

Fig. 9 The relationship between mean relative difference (*MRD*) and standard deviation of relative difference (*SDRD*) of soil salinity for **a** temporal stability analysis and **b** improved temporal stability analysis. Solid dots are results of representative locations with the minimum SDRD

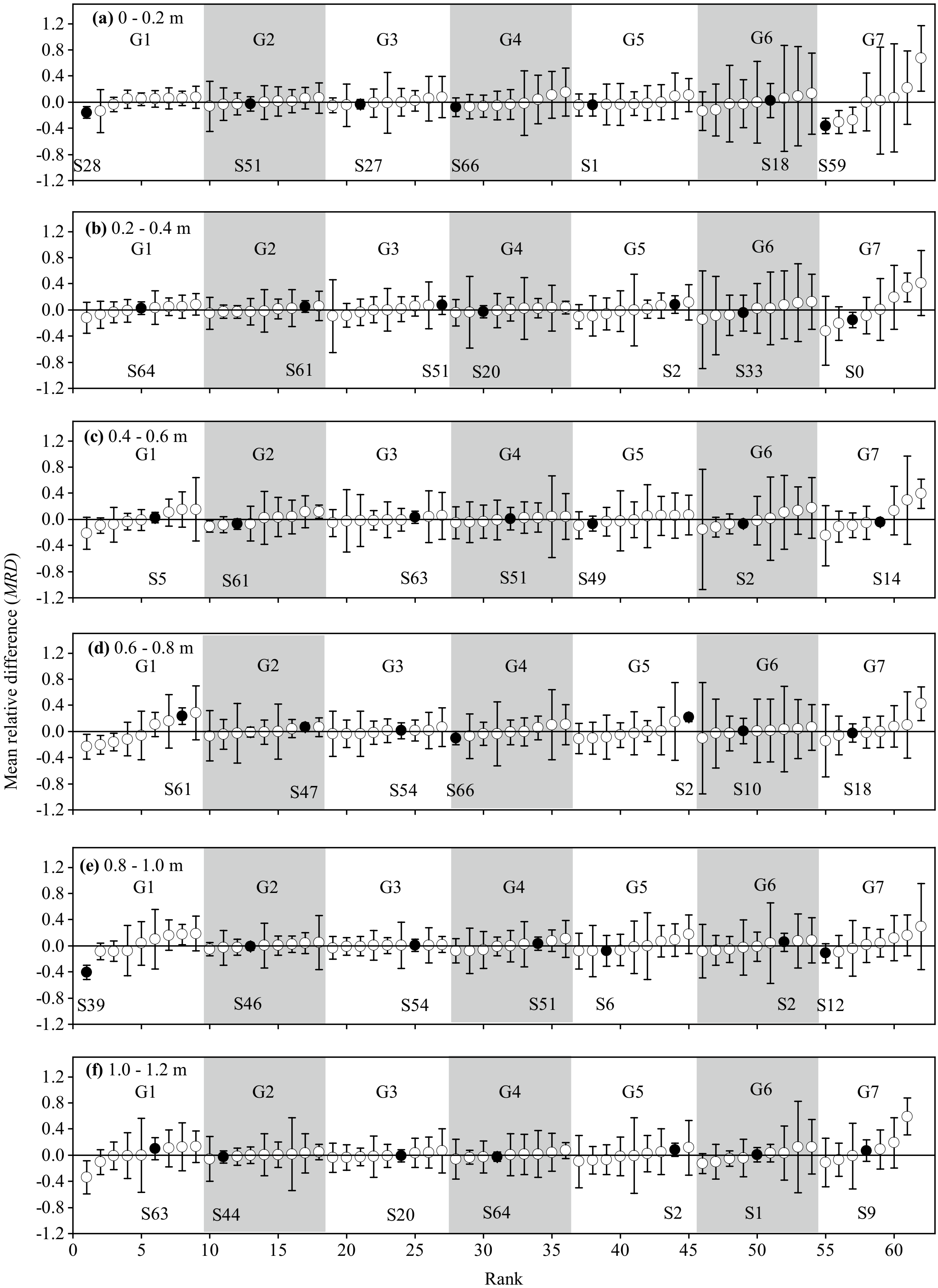
(a) 0 - 0.2 m
G1
G2
G3
G4
G5
G6
G7
S28
S51
S27
S66
S1
S18
S59
(b) 0.2 - 0.4 m
S64
S61
S51
S20
S2
S33
S0
(c) 0.4 - 0.6 m
S5
S61
S63
S51
S49
S2
S14
(d) 0.6 - 0.8 m
S61
S47
S54
S66
S2
S10
S18
(e) 0.8 - 1.0 m
S39
S46
S54
S51
S6
S2
S12
(f) 1.0 - 1.2 m
S63
S44
S20
S64
S2
S1
S9
Mean relative difference (MRD)
Rank

◂**Fig. 10** The mean relative difference (*MRD*) and standard deviation of relative difference (*SDRD*) of soil salinity at different soil layers in each group. G1–G7 are groups for improved temporal stability, and the S28, S51, …, S9 are the representative locations in each group, respectively

3.3 Estimating the soil salinity means with temporal stability analysis

Considering that soil salinity data within the depth of 1.2–1.8 m at some sampling locations were missing due to shallow water table in early May, only the soil salinity data within the depth of 0–1.2 m was used for temporal stability analysis. The *MRD* and *SDRD* of soil salinity are shown in Fig. 7. The variation ranges of *MRD* of soil salinity at the soil layers of 0–0.2 m, 0.2–0.4 m, 0.4–0.6 m, 0.6–0.8 m, 0.8–1.0 m, and 1.0–1.2 m were − 0.54–2.91, − 0.53–1.90, − 0.63–1.87, − 0.63–1.61, − 0.70–1.49, and − 0.63–1.86, respectively. The corresponding *SDRD* of soil salinity at different soil layers were 0.06–2.78, 0.04–1.34, 0.03–1.44, 0.03–1.44, 0.04–1.34, and 0.02–1.03. The sample location in each soil layer with the minimum *SDRD* was chosen as the representative location to predict the mean soil salinity. The predicted and measured soil salinity for the 4 sampling times are showed in Fig. 8a. However, the *MRE* values were − 6.47 to 7.2%, *RMSE* values 0.02 to 0.03 dS/m, and R^2 values 0.33 to 0.84, which show that it is difficult to estimate the spatial mean of soil salinity by the temporal stability analysis.

The reason causing the unsatisfactory predictions is attributed to the strong variability of soil salinity. The *MRD* of soil salinity in this study area are much larger than *MRD* of soil water content with most ranging from − 0.5 to 0.6 (Brocca et al. 2009), and also larger than *MRD* of soil salinity in field scale ranging from − 0.75 to 1.11 (Douaik et al. 2006). It demonstrates that larger variation of soil salinity is found in the study area. In addition, the *SDRD* of soil salinity are also much larger than those of soil water content with maximum values smaller than 0.50 (Brocca et al. 2009), and also larger than that of soil salinity in field scales ranging from 0.14 to 0.53 (Douaik et al. 2006). It can also be found that the *SDRD* of soil salinity became larger with the increase of *MRD* as shown in Fig. 9a. The changes of soil salinity are highly related to its value (Sun et al. 2019), and thus the temporal stability analysis can provide accurate results when the sample location with the minimum *SDRD* value and meanwhile owning the *MRD* close to 0 existed. However, in this area, the sample location with the *MRD* close to 0 owning to relatively large *SDRD*, and the sample location with the minimum *SDRD* owning to relatively large negative *MRD* as shown in Fig. 9a. Therefore, the temporal stability analysis should be improved in this area for more accurate prediction of spatial mean of soil salinity.

3.4 Estimating the spatial mean soil salinity with the improved temporal stability analysis

The 62 sampling locations were divided into 7 groups according to ranked *MRD* from small to large as shown in Fig. 7, and each of the first 6 groups have 9 sampling locations, and the 7-th group has 8 sampling locations. The data of 62 sampling locations while not 68 sampling locations were used for temporal stability analysis since there were 6 sampling locations not be collected due to irrigation events at all sampling times. The *MRD* and *SDRD* values in each group calculated by the temporal stability analysis are shown in Fig. 10. The *MRD* ranged from − 0.41 to 0.67, and most were between − 0.20 and 0.20. It can be found that the improved temporal stability

Table 3 Representative locations and its mean relative difference (*MRD*) at different soil layers of each group obtained by the improved temporal stability analysis

Soil layer		G1	G2	G3	G4	G5	G6	G7
0–0.2 m	Location	S28	S51	S27	S66	S1	S18	S59
	MRD	− 0.158	− 0.023	− 0.032	− 0.074	− 0.042	0.027	-0.365
0.2–0.4 m	Location	S64	S61	S51	S20	S2	S33	S0
	MRD	0.028	0.051	0.073	− 0.027	0.079	− 0.047	− 0.153
0.4–0.6 m	Location	S5	S61	S63	S51	S49	S2	S14
	MRD	0.025	− 0.072	0.031	0.010	− 0.065	− 0.066	− 0.047
0.6–0.8 m	Location	S61	S47	S54	S66	S2	S10	S18
	MRD	0.236	0.063	0.014	− 0.100	0.214	0.007	− 0.025
0.8–1.0 m	Location	S39	S46	S54	S51	S6	S2	S12
	MRD	− 0.406	− 0.014	0.006	0.031	− 0.077	0.055	− 0.115
1.0–1.2 m	Location	S63	S44	S20	S64	S2	S1	S9
	MRD	0.099	− 0.029	− 0.008	− 0.024	0.085	0.008	0.067

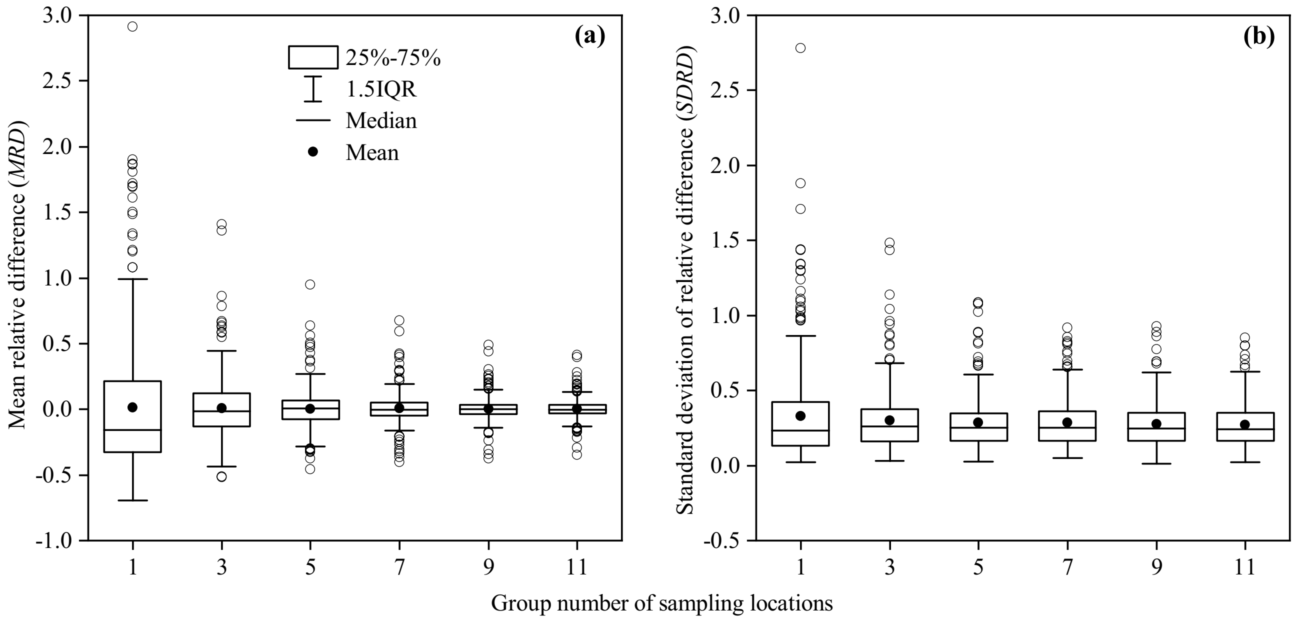

Fig. 11 The mean relative difference (*MRD*) and standard deviation of relative difference (*SDRD*) of soil salinity with different groups of sampling locations

analysis reduced variation of soil salinity in each group greatly. Similarly, the *SDRD* in each group with improved temporal stability analysis were also decreased greatly with most of them smaller than 0.5. The relationship between *SDRD* and *MRD* with improved temporal stability analysis is shown in Fig. 9b. The representative locations with minimum *SDRD* were also the ones whose *MRD* were close to 0, which implies that more reasonable representative locations for soil salinity are obtained by the improved temporal stability analysis. The representative location of each group with the minimum *SDRD* at different soil layers is listed in Table 3. The representative locations in different soil layer were different, which indicates that it is difficult to find a location to estimate the average soil salinity at different soil layers simultaneously. This is consistent with the temporal stability analysis of soil water content reported in literatures (Gao et al. 2013a; Guber et al. 2008; Heathman et al. 2012; Hu et al. 2010). The predicted and measured mean soil salinities at the 4 sampling times are shown in Fig. 8b. The *MRE* values were − 2.72 to 1.61%, *RMSE* values 0.04 to 0.05 dS/m, and R^2 values larger than 0.90, which demonstrate the good performance of improved temporal stability analysis in predicting soil salinity means. As a summary, it is important to decrease the *MRD* and *SDRD* of soil salinity to improve the effectiveness of temporal stability analysis. It would be an effective way to divide the sampling locations into several groups to find the representative locations in areas with strong variability of soil salinity.

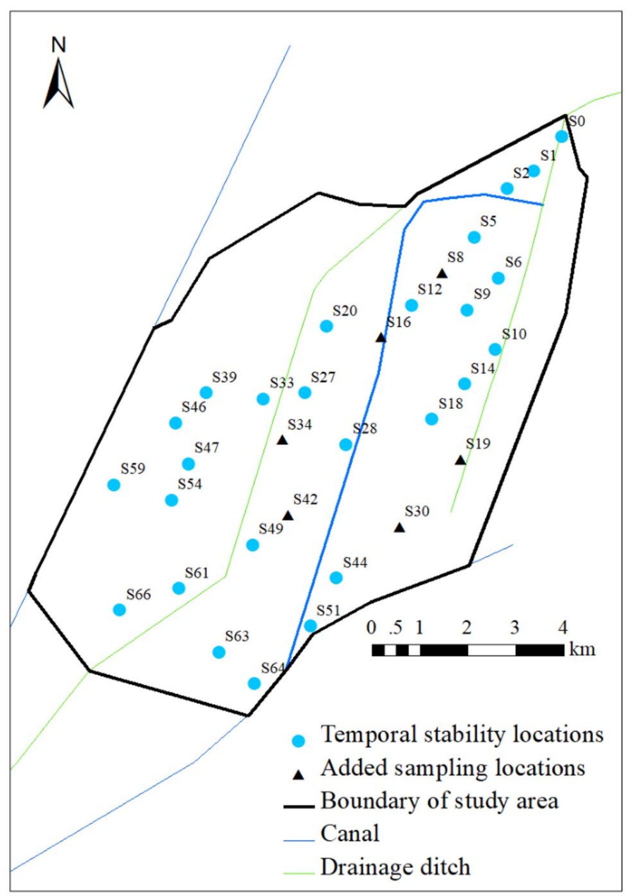

Fig. 12 The sampling locations for long-term soil salinity monitoring

Table 4 The semivariogram models and parameters of root zone (within the depth of 0–0.6 m) and 0.6–1.2 m layer soil salinity for all sampling locations and 32 representative sampling locations

	Soil layer	Time	Model	C_0	C_0+C_1	$C_0/(C_0+C_1)$	R (m)
All sampling locations	0–0.6 m	Y1705	Spherical	0.0001	0.2682	0.04	1620
		Y1709	Spherical	0.0135	0.2900	4.66	1730
		Y1805	Gaussian	0.0001	0.1872	0.05	1593
		Y1809	Exponential	0.0990	0.5510	17.97	37,470
	0.6–1.2 m	Y1705	Gaussian	0.0346	0.2112	16.38	1784
		Y1709	Exponential	0.0968	0.2826	34.25	17,970
		Y1805	Exponential	0.0482	0.2554	18.87	5820
		Y1809	Spherical	0.1053	0.3306	31.85	9590
32 representative sampling locations	0–0.6 m	Y1705	Spherical	0.0001	0.2952	0.03	2050
		Y1709	Spherical	0.0001	0.2712	0.04	2260
		Y1805	Gaussian	0.0001	0.1682	0.06	1611
		Y1809	Exponential	0.0702	0.3844	18.26	14,370
	0.6–1.2 m	Y1705	Gaussian	0.0001	0.2582	0.04	1697
		Y1709	Exponential	0.0693	0.3696	18.75	24,480
		Y1805	Exponential	0.0585	0.2600	22.50	8100
		Y1809	Spherical	0.1064	0.3188	33.38	9470

C_0 nugget variance, C_0+C_1 sill variance, $C_0/(C_0+C_1)$ degree of spatial dependence (%), R range

3.5 Discussion for dividing the sampling locations into groups using the improved temporal stability analysis

To investigate the impact of dividing the sampling locations into groups when using the improved temporal stability analysis for soil salinity prediction, six schemes by dividing the 62 sampling locations into 1, 3, 5, 7, 9, and 11 groups were carried out. It should be noted that the results corresponding to one group is the same as those of the temporal stability analysis discussed in Sect. 3.3. The predicted and measured soil salinity and the evaluation indictors for the 4 sampling times under the six group schemes are shown in Fig. 8. It can be found that predicted soil salinity under different group numbers ranging from 3 to 11 are significantly improved comparing to temporal stability analysis. The *MRE* of soil salinity with 3 to 11 groups ranged from − 2.72 to 1.75%, *RMSE* from 0.02 to 0.08 dS/m, and R^2 from 0.84 to 0.98 with most R^2 values larger than 0.90. These results indicate that dividing sampling locations into more groups can obtain more accurate range of soil salinity as shown in Fig. 8. However, increasing the group number cannot further improve the prediction results when considering the almost identical evaluation indicators of predicted soil salinity as shown in Fig. 8b–f.

The changes of *MRD* and *SDRD* of soil salinity under the six group schemes are shown in Fig. 11 a and b. The range of *MRD* decreased with increasing of the group number. The range of *SDRD* decreased obviously when the group number increased from 1 to 7, and then remained unchanged when the group number was greater than 7. Thus, it is recommended that dividing the sampling locations into 7 groups for the study area is suitable. When using the temporal stability analysis, the *MRD* and *SDRD* values under different group scheme should be evaluated to determine the group number.

3.6 Long-term soil salinity sampling locations

The key to effective and efficient long-term soil salinity monitoring is to establish an effective monitoring network with minimal cost to obtain the major soil salt data (Baalousha 2010), which can be used to evaluate long-term evolution characteristics of soil salinity in time and space. Because the spatial pattern of soil salinity at different soil layers in depth of 1.2–1.8 m is similar to that of 0.6–1.2 m, sampling depth in this area was determined to be 0–1.2 m. There were 7 representative locations in every layer, and totally there were 26 representative locations as shown in Table 3. In addition, to have even distribution of the sampling locations, another 6 sampling locations, i.e., S8, S16, S19, S30, S34, and S42, were added. The sampling locations in monitoring network are shown in Fig. 12, including 32 locations.

As listed in Table 4, the semivariogram models and parameters of root zone (within the depth of 0–0.6 m)

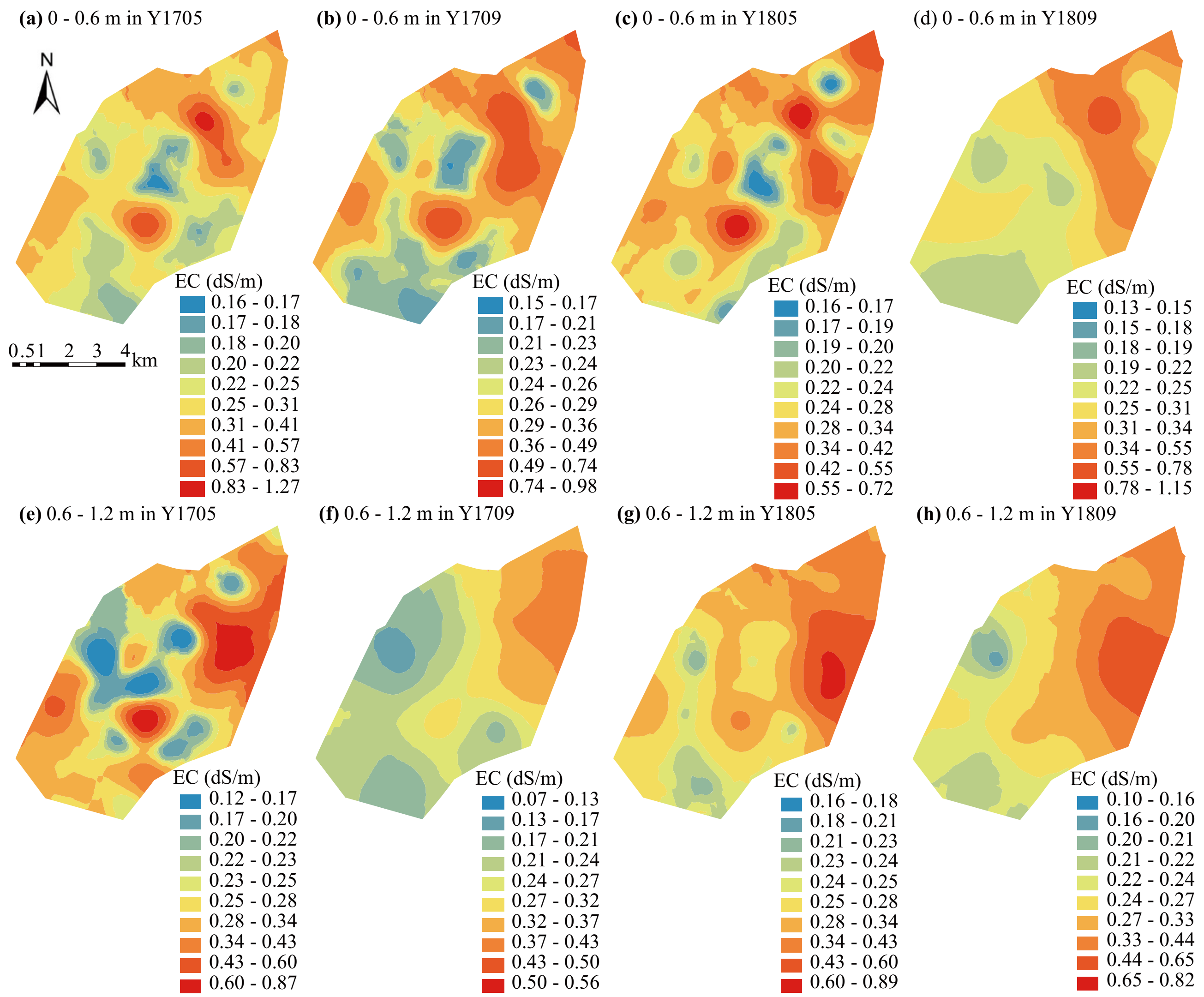

Fig. 13 The spatial distribution of root zone (within the depth of 0–0.6 m) and 0.6–1.2 m layer soil salinity determined by sampling locations for long-term soil salinity monitoring at the 4 sampling times

and 0.6–1.2 m layer soil salinity obtained by the 32 sampling locations were close to that determined for all sampling locations. The distribution of root zone soil salinity determined by the 32 sampling locations is shown in Fig. 13a–d, which shows a pattern similar to that obtained by using all sampling locations as shown in Fig. 6a–d. The area of different root zone soil salinity determined by the 32 sampling locations and all sampling locations are shown in Fig. 14a–d, with the *MRE* ranging from − 20.78 to 2.36%, and most R^2 more than 0.75. The above results indicate that the spatial distribution of root zone soil salinity can be determined by the representative sampling locations. For 0.6–1.2 m soil layer, the spatial distribution of soil salinity in Y1705, Y1709, and Y1805 determined by the 32 sampling locations (Fig. 13e–g) were also close to that obtained by all sampling locations (Fig. 6e–g). The *MRE* between area of different soil salinity determined by the 32 sampling locations and all sampling locations in Y1705, Y1709, and Y1805 ranged from − 23.67 to 13.70%, and R^2 from 0.46 to 0.88. Only relatively poor results were found for the area with soil salinity being smaller than 0.21 dS/m in Y1809, which would be caused by sparse points. In general, the spatial distribution of soil salinity determined by the 32 representative sampling locations are acceptable in the study area.

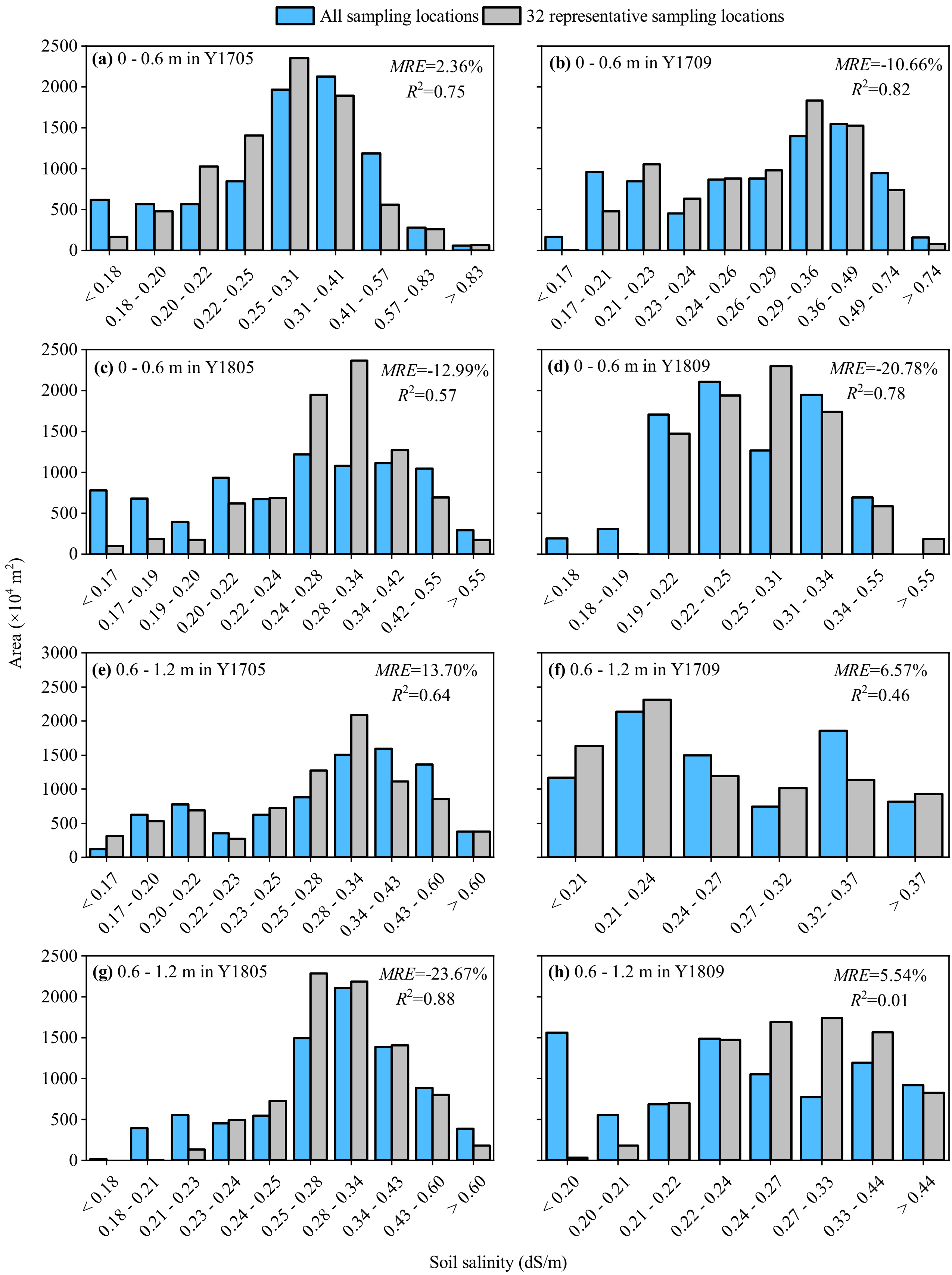

Fig. 14 The area of different soil salinity determined by 32 representative sampling locations and all sampling locations

4 Conclusions

In this study, a 2-year field experiment was carried out to characterize the temporal and spatial variability of soil salinity in a large irrigation area in northern China. The temporal stability analysis was improved to estimate and predict the spatial mean of soil salt in this area. A monitoring network for this area was then recommended to evaluate the long-term evolution characteristics of soil salinity by comprehensively considering the results of spatiotemporal variability and the improved temporal stability analysis. The major conclusions were drawn as follows:

1. Regional averaged soil salinity dynamics have obvious seasonal variation characteristics. The spatial dependency of soil salinity is strong in study area. The spatial distribution of soil salinity is similar among different soil layers and relatively stable in time.

2. It is difficult to use temporal stability analysis for estimating the spatial mean of soil salinity due to the strong variability of soil salinity with larger range of *MRD* and *SDRD*.

3. Dividing the sampling locations into several groups can decrease the range of *MRD* and *SDRD* in each group, and can significantly improve the prediction accuracy of soil salinity.

4. When using temporal stability analysis, the *MRD* and *SDRD* values under different group schemes should be evaluated to determine the group number. It should be required that the representative sampling location with minimum *SDRD* owns the *MRD* close to 0 in each group.

5. The number of sampling locations to evaluate long-term evolution characteristics of soil salinity in time and space is 32 for the study area, which are comprehensively considered by the results of spatiotemporal variability and the improved temporal stability analysis.

Acknowledgements We thank the editor and anonymous reviewers for their very helpful comments and revision of the manuscript.

Author contribution All authors contributed to the study conception and design. Material preparation and study method were performed by Guanfang Sun, Yan Zhu, Ming Ye, and Jinzhong Yang. Data collection and analysis were performed by Guanfang Sun, Yang Yang, Wei Mao, and Jingwei Wu. The first draft of the manuscript was written by Guanfang Sun, and all authors commented on previous versions of the manuscript. All authors read and approved the final manuscript.

Funding The study was partially supported by the Natural Science Foundation of China through Grants (51779178, 51790532, and 52009094) and the project of water conservancy science and technology plan in Inner Mongolia Autonomous Region (Grant No. 213–03-99–303002-NSK2017-M1).

Data availability The datasets used and/or analyzed during the current study are available from the corresponding author on reasonable request.

Code availability Not applicable.

Declarations

Conflict of interest The authors declare no competing interests.

References

Abd-Elgawad M, Shendi MM, Sofi DM, Abdurrahman HA, Ahmed AM (2013) Geographic distribution of soil salinity, alkalinity and calcicity within Fayoum and Tamia Districts, Fayoum Governorate, Egypt. In: Developments in Soil Salinity Assessment and Reclamation. Springer, Netherlands

Akramkhanov A, Martius C, Park SJ, Hendrickx JMH (2011) Environmental factors of spatial distribution of soil salinity on flat irrigated terrain. Geoderma 163:55–62

Baalousha H (2010) Assessment of a groundwater quality monitoring network using vulnerability mapping and geostatistics: A case study from Heretaunga Plains, New Zealand. Agric Water Manage 97:240–246

Bilgili AV (2013) Spatial assessment of soil salinity in the Harran Plain using multiple kriging techniques. Environ Monit Assess 185:777–795

Brocca L, Melone F, Moramarco T, Morbidelli R (2009) Soil moisture temporal stability over experimental areas in Central Italy. Geoderma 148:364–374

Castrignanò A, Lopez G, Stelluti M (1994) Temporal and spatial variability of electrical conductivity, Na content and sodium adsorption ratio of soil saturation extract measurements. Eur J Agron 3:221–226

Corwin DL, Lesch SM, Oster JD, Kaffka SR (2006) Monitoring management-induced spatio-temporal changes in soil quality through soil sampling directed by apparent electrical conductivity. Geoderma 131:369–387

Daliakopoulos IN, Tsanis IK, Koutroulis A, Kourgialas NN, Varouchakis AE, Karatzas GP, Ritsema CJ (2016) The threat of soil salinity: A European scale review. Sci Total Environ 573:727–739

Ding JL, Yu DL (2014) Monitoring and evaluating spatial variability of soil salinity in dry and wet seasons in the Werigan-Kuqa Oasis, China, using remote sensing and electromagnetic induction instruments. Geoderma 235–236:316–322

Douaik A, Meirvenne MV, Tã3Th T (2006) Temporal stability of spatial patterns of soil salinity determined from laboratory and field electrolytic conductivity. Arid Soil Res Rehab 20:1-13

Douaik A, Van Meirvenne M, Tóth T (2005) Soil salinity mapping using spatio-temporal kriging and Bayesian maximum entropy with interval soft data. Geoderma 128:234–248

Douaik A, Van Meirvenne M, Tóth T (2007) Statistical methods for evaluating soil salinity spatial and temporal variability. Soil Sci Soc Am J 71:1629–1635

Elprince AM (2013) Spatial analysis using a proportional effect semi-variogram. In: Developments in Soil Salinity Assessment and Reclamation. Springer, Netherlands

Florinsky IV, Eilers RG, Manning GR, Fuller LG (2002) Prediction of soil properties by digital terrain modelling. Environ Modell Softw 17:295–311

Foley JA, Defries R, Asner GP, Barford C, Bonan G, Carpenter SR, Chapin FS, Coe MT, Daily GC, Gibbs HK, Helkowski JH, Holloway T, Howard EA, Kucharik CJ, Monfreda C, Patz JA, Prentice IC, Ramankutty N, Snyder PK (2005) Global consequences of land use. Science 309:570–574

Gao XD, Wu PT, Zhao XN, Wang JW, Shi YG, Zhang BQ, Tian L, Li HB (2013a) Estimation of spatial soil moisture averages in a large gully of the Loess Plateau of China through statistical and modeling solutions. J Hydrol 486:466–478

Gao XD, Wu PT, Zhao XN, Zhang BQ, Wang JW, Shi YG (2013b) Estimating the spatial means and variability of root-zone soil moisture in gullies using measurements from nearby uplands. J Hydrol 476:28–41

Gasch CK, Hengl T, Meyer GB, H, Magney TS, Brown DJ, (2015) Spatio-temporal interpolation of soil water, temperature, and electrical conductivity in 3D + T: The Cook Agronomy Farm data set. Spat Stat 14:70–90

Grayson RB, Western AW (1998) Towards areal estimation of soil water content from point measurements: time and space stability of mean response. J Hydrol 207:68–82

Guber AK, Gish TJ, Pachepsky YA, Genuchten MTV, Daughtry CST, Nicholson TJ, Cady RE (2008) Temporal stability in soil water content patterns across agricultural fields. CATENA 73:125–133

Hajrasuliha S, Baniabbassi N, Metthey J, Nielsen DR (1980) Spatial variability of soil sampling for salinity studies in Southwest Iran. Irrig Sci 1:197–208

Hamzehpour N, Eghbal MK, Bogaert P, Toomanian N, Sokouti RS (2013) Spatial prediction of soil salinity using kriging with measurement errors and probabilistic soft data. Arid Land Res Manag 27:128–139

Heathman GC, Cosh MH, Han E, Jackson TJ, Mckee L, Mcafee S (2012) Field scale spatiotemporal analysis of surface soil moisture for evaluating point-scale in situ networks. Geoderma 170:195–205

Hu W, Shao MA, Han FP, Reichardt K (2011) Spatio-temporal variability behavior of land surface soil water content in shrub- and grass-land. Geoderma 162:260–272

Hu W, Shao MA, Han FP, Reichardt K, Tan J (2010) Watershed scale temporal stability of soil water content. Geoderma 158:181–198

Jacobs JM, Hsu EC, Choi M (2010) Time stability and variability of electronically scanned thinned array radiometer soil moisture during Southern Great Plains hydrology experiments. Hydrol Process 24:2807–2819

Juan P, Mateu J, Jordan MM, Mataix-Solera J, Meléndez-Pastor I, Navarro-Pedreño J (2011) Geostatistical methods to identify and map spatial variations of soil salinity. J Geochem Explor 108:62–72

Li HY, Shi Z, Webster R, Triantafilis J (2013) Mapping the three-dimensional variation of soil salinity in a rice-paddy soil. Geoderma 195–196:31–41

Li J, Wan HY, Shang SH (2020) Comparison of interpolation methods for mapping layered soil particle-size fractions and texture in an arid oasis. Catena 190:104514

Lin HS (2006) Temporal stability of soil moisture spatial pattern and subsurface preferential flow pathways in the shale hills catchment. Vadose Zone J 5:317–340

Liu BX, Shao MA (2014) Estimation of soil water storage using temporal stability in four land uses over 10 years on the Loess Plateau, China. J Hydrol 517:974–984

Mohanty BP, Skaggs TH (2001) Spatio-temporal evolution and time-stable characteristics of soil moisture within remote sensing footprints with varying soil, slope, and vegetation. Adv Water Resour 24:1051–1067

Navarro-Pedreño J, Jordan MM, Meléndez-Pastor I, Gómez I, Juan P, Mateu J (2007) Estimation of soil salinity in semi-arid land using a geostatistical model. Land Degrad Devlop 18:339–353

Panagopoulos T, Jesus J, Antunes MDC, Beltrão J (2006) Analysis of spatial interpolation for optimising management of a salinized field cultivated with lettuce. Eur J Agron 24:1–10

Penna D, Brocca L, Borga M, Fontana GD (2013) Soil moisture temporal stability at different depths on two alpine hillslopes during wet and dry periods. J Hydrol 477:55–71

Ren DY, Xu X, Hao YY, Huang GH (2016) Modeling and assessing field irrigation water use in a canal system of Hetao, upper Yellow River basin: application to maize, sunflower and watermelon. J Hydrol 532:122–139

Ruybal CJ, Hogue1 TS, McCray JE (2019) Evaluation of groundwater levels in the arapahoe aquifer using spatiotemporal regression kriging. Water Resour Res 55:2820-2837

Scudiero E, Skaggs TH, Corwin DL (2017) Simplifying field-scale assessment of spatiotemporal changes of soil salinity. Sci Total Environ 587–588:273–281

Shahabi M, Jafarzadeh AA, Neyshabouri MR, Ghorbani MA, Valizadeh Kamran K (2016) Spatial modeling of soil salinity using multiple linear regression, ordinary kriging and artificial neural network methods. Arch Agron Soil Sci 63:151–160

Singh A (2015) Soil salinization and waterlogging: a threat to environment and agricultural sustainability. Ecol Indic 57:128–130

Sun GF, Zhu Y, Ye M, Yang JZ, Qu ZY, Mao W, Wu JW (2019) Development and application of long-term root zone salt balance model for predicting soil salinity in arid shallow water table area. Agric Water Manage 213:486–498

Sylla M, Stein A, Van BN, Fresco LO (1995) Spatial variability of soil salinity at different scales in the mangrove rice agro-ecosystem in West Africa. Agric Ecosyst Environ 54:1–15

Utset A, Ruiz ME, Herrera J, de Leon DP (1998) A geostatistical method for soil salinity sample site spacing. Geoderma 86:143–151

Vachaud G, Silans APD, Balabanis P, Vauclin M (1985) Temporal stability of spatially measured soil water probability density function. Soil Sci Soc Am J 49:822–828

Vanderlinden K, Vereecken H, Hardelauf H, Herbst M, Martínez G, Cosh MH, Pachepsky YA (2012) Temporal stability of soil water contents: A review of data and analyses. Vadose Zone J 11:1–19

Visconti F, de Paz JM, Rubio JL (2010) What information does the electrical conductivity of soil water extracts of 1 to 5 ratio (w/v) provide for soil salinity assessment of agricultural irrigated lands? Geoderma 154:387–397

Walter C, McBratney AB, Donuaoui A, Minasny B (2001) Spatial prediction of topsoil salinity in the Chelif Valley, Algeria, using local ordinary kriging with local variograms versus whole-area variogram. Soil Res 39:259–272

Wang YG, Deng CY, Liu Y, Niu ZR, Li Y (2018) Identifying change in spatial accumulation of soil salinity in an inland river watershed, China. Sci Total Environ 621:177–185

Wang ZR, Zhao GX, Gao MX, Chang CY (2017) Spatial variability of soil salinity in coastal saline soil at different scales in the Yellow River Delta, China. Environ Monit Assess 189:1–12

Warrick AW, Nielsen DR (1980) Spatial variability of soil physical properties in the field. In: Applications of Soil Physics. Academic Press, New York

Webster R, Oliver MA (2007) Geostatistics for environmental scientists, Second Edition. John Wiley & Sons, Ltd

Wichelns D, Oster JD (2006) Sustainable irrigation is necessary and achievable, but direct costs and environmental impacts can be substantial. Agric Water Manage 86:114–127

Wu WY, Yin SY, Liu HL, Niu Y, Bao Z (2014) The geostatistic-based spatial distribution variations of soil salts under long-term wastewater irrigation. Environ Monit Assess 186:6747–6756

Xing XG, Zhao WG, Ma XY, Zhao W, Shi WJ (2015) Temporal stability of soil salinity in root zone of cotton under drip irrigation with plastic mulch (in Chinese). Transactions of the CSAE 46:147–153

Zare-Mehrjardi M, Taghizadeh-Mehrjardp R, Akbarzadeh A (2010) Evaluation of geostatistical techniques for mapping spatial distribution of soil PH, salinity and plant cover affected by environmental factors in southern Iran. Not Sci Biol 2:92–103

Zhang RD (2005) Theory and application of spatial variability. Science Press, Beijing (in Chinese)

Zheng Z, Zhang FR, Ma FY, Chai XR, Zhu ZQ, Shi JL, Zhang SX (2009) Spatiotemporal changes in soil salinity in a drip-irrigated field. Geoderma 149:243–248

Zhou HH, Chen YN, Li WH (2010) Soil properties and their spatial pattern in an oasis on the lower reaches of the Tarim River, northwest China. Agric Water Manage 97:1915–1922